

# Analysis Technique of Millimeter-Wave Propagating Modes in an Oversized Corrugated Waveguide Using Developed Beam Profile Monitors<sup>\*</sup>)

Takashi SHIMOZUMA<sup>1)</sup>, Sakuji KOBAYASHI<sup>1)</sup>, Satoshi ITO<sup>1)</sup>, Kohta OKADA<sup>2)</sup>, Yasuhiko ITO<sup>1)</sup>, Yasuo YOSHIMURA<sup>1)</sup>, Hiroe IGAMI<sup>1)</sup>, Hiromi TAKAHASHI<sup>1)</sup>, Toru TSUJIMURA<sup>1)</sup>, Yoshinori MIZUNO<sup>1)</sup> and Shin KUBO<sup>1,2)</sup>

<sup>1)</sup>National Institute for Fusion Science, National Institutes of Natural Sciences, 322-6 Oroshi-Cho, Toki-City, Gifu 509-5292, Japan

<sup>2)</sup>Nagoya University, Furo-Cho, Chikusa-Ku, Nagoya 464-8601, Japan

(Received 28 December 2017 / Accepted 16 March 2018)

A mode analysis technique of the millimeter-wave which propagates in the corrugated waveguide of the electron cyclotron resonance heating (ECRH) transmission line is proposed. The technique is based on the signals detected by beam-profile monitors (BPMs) developed and installed in the reflection plane mirror of the miterbends in the ECRH transmission line. The developed BPM consists of a mirror plate, Peltier-device array, and a heat-sink. The voltage signal of each Peltier device is related with the temperature of the mirror surface. The program which can analyze propagating-mode components using these signals is developed. The possibility of the propagating mode analyses using this code was confirmed using the artificially synthesized model data on the miterbend reflector.

© 2018 The Japan Society of Plasma Science and Nuclear Fusion Research

Keywords: electron cyclotron resonance heating, mode analysis, corrugated waveguide, gyrotron, millimeter wave

DOI: 10.1585/pfr.13.3405036

## 1. Introduction

In a high-power Electron Cyclotron Resonance Heating (ECRH) system for plasma heating, a long-distance and low-loss transmission system of the millimeter-wave (mmw) is required. In the ECRH system of the Large Helical Device (LHD) of National Institute for Fusion Science (NIFS), the total length of the transmission line (TL) is 70 - 100 m, and the transmission efficiency is about 80 - 90 % as shown in Table 1. The TL system, which is composed of corrugated-waveguides and miterbends, is precisely aligned by using a He-Ne laser beam. The transmission loss is mainly caused by the misalignment of the mmw generated by a gyrotron to the TL. Accordingly, the correct coupling of the mmw beam to the corrugated waveguide is required at the waveguide entrance. We have developed a power profile monitor of the mmw beam propagating in the evacuated corrugated waveguide in real-time [1]. The beam profile monitor (BPM) consists of an mmw reflector, a Peltier-device array and a heat-sink. A proto-type BPM was constructed and tested using high power mmws. These results show that the BPM can be used as a real-time power profile monitor of the high power mmw in the TLs. Here, we propose a technique to analyze the propagating modes using the signals of plural BPMs installed in the

author's e-mail: shimozuma.takashi@nifs.ac.jp

<sup>\*</sup>) This article is based on the presentation at the 26th International Toki Conference (ITC26).

Table 1 Summary of the ECRH System in LHD.

| Line No.                  | #1        | #2        | #4        | #5        | #7        | #11  |
|---------------------------|-----------|-----------|-----------|-----------|-----------|------|
| <b>Gyrotrons</b>          |           |           |           |           |           |      |
| Freq. (GHz)               | 77        | 77        | 154       | 154       | 77        | 82.7 |
| Power (MW)                | 1.5 (0.3) | 1.2 (0.3) | 1.0 (0.5) | 1.0 (0.5) | 1.0 (0.3) | 0.45 |
| Pulse (s)                 | <2 (CW)   | <10 (CW)  | <5 (CW)   | <5 (CW)   | <5 (CW)   | <2   |
| <b>Transmission Lines</b> |           |           |           |           |           |      |
| Length (m)                | 90        | 90        | 70        | 90        | 100       | 110  |
| Diameter (mm)             | 88.9      | 88.9      | 88.9      | 88.9      | 88.9      | 88.9 |
| Trans. Effi. (%)          | 82        | 81        | 91        | -         | 85        | 82   |
| <b>Antennas</b>           |           |           |           |           |           |      |
| Number of mirrors         | 4         | 3         | 2         | 2         | 2         | 4    |

miterbends of the ECRH transmission line.

In this paper, the structure of the BPM and the total measurement system are shown in Section 2. In Section 3, the procedure of mode analyses based on the BPM data is explained based on the similar algorithm in [2]. In Section 4, the analyzed results of the mode contents are shown for the artificially synthesized mode patterns which take into account several lower-order modes. Finally, Section 5 will be devoted to the summary.

## 2. Structure of a BPM and Total Measurement System

The structure of a BPM proposed is schematically shown in Fig. 1. A two-dimensional array of Peltier-

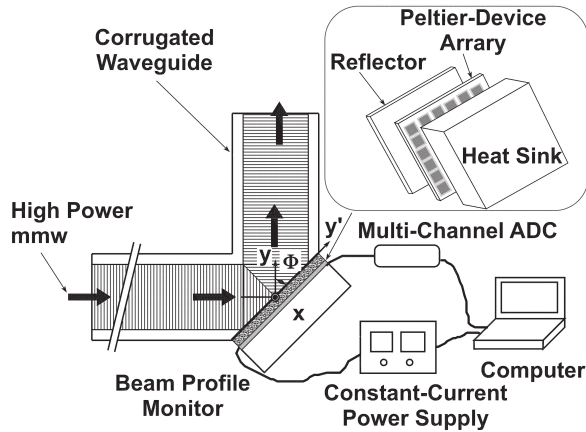


Fig. 1 Millimeter-wave power profile monitor system installed in an ECRH transmission line.

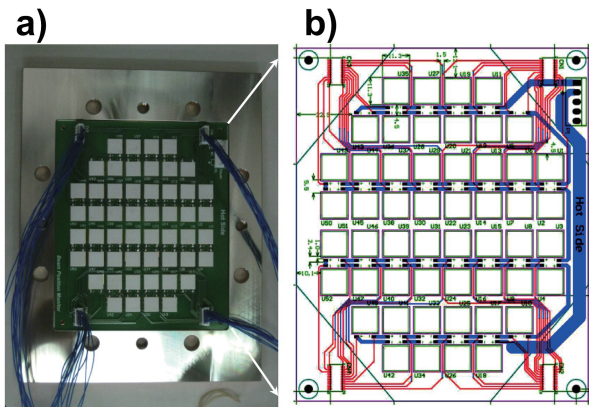


Fig. 2 a) A photograph of the BPM installed on the air-side of a miterbend reflector without a heat-sink, and b) a layout drawing of Peltier-devices and double-sided printed circuits. The blue lines are serially connected current circuits, and the red lines show the lines for voltage measurement of each Peltier device. Those are independently connected to the insulated multi-channel A/D converters to measure the voltage of each Peltier device.

devices is aligned and installed on the atmospheric side of a thin miterbend reflector with a water-cooled heat-sink. An mmw beam propagating in the corrugated waveguide is reflected on the mirror surface of the miterbend and partly absorbed in the reflector plate. The generated heat by Ohmic loss of the electromagnetic wave diffuses to the atmospheric side of the reflector and is removed by the Peltier-devices. The voltage of each Peltier-device is approximately expressed as the following equation.

$$V = IR + S(T_H - T_C), \quad (1)$$

where  $I$ ,  $R$ , and  $S$  are electric current, resistance, and Seebeck coefficient of the Peltier-device, respectively.  $T_H$  and  $T_C$  represent hot-side (heat-sink side) and cold-side (reflector side) temperature of the Peltier-device. When these Peltier-devices are connected serially and driven by the constant current control ( $I = \text{constant}$ ), the voltage change of each device is almost linearly proportional to the tem-

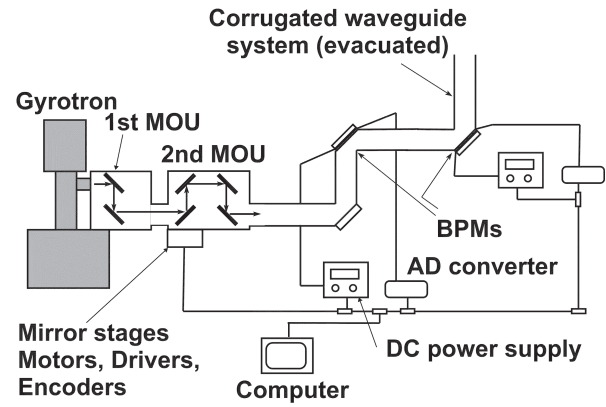


Fig. 3 Schematic view of the total system for high power mmw beam alignment installed in an ECRH transmission line.

perature change of the cold-side of the device, if the temperature at the hot-side of the Peltier-device is kept constant. The information of the two-dimensional temperature profile of the miterbend reflector can give the real-time information of the position and the profile of the mmw beam. The photograph and circuits of the constructed BPM are shown in Fig. 2, a) the photograph of BPM without a heat-sink and b) a layout drawing of Peltier-devices and double-sided printed circuits.

A schematic view of the alignment system installed in the ECRH transmission line system is illustrated in Fig. 3. In the TL, two or more BPMs will be installed in the miterbends. Based on the BPM signals, propagating modes are analyzed, and then the mirrors in the 2nd matching optics unit (MOU) are feedback controlled so that the propagating mode becomes the fundamental  $HE_{11}$  mode ( $LP_{01}$  mode).

### 3. Technique of Mode Analysis Based on the BPM Data

We consider a mode analysis technique using the 2-dimensional BPM signals based on the almost the same manner as described in [2].

For simplicity, linear polarized (LP) modes in a circular corrugated waveguide are considered. The electric fields of the LP-(e) and -(o) modes, in which (e) and (o) mean even and odd, respectively, are expressed as the following equations [3]:

$$LP_{nm}^y(e) : \mathbf{E}_{\perp\sigma}(r, \theta) = \hat{y} \sqrt{2} f_{\sigma} J_n(X_{\sigma} r/a) \cos(n\theta), \quad (2)$$

$$LP_{nm}^y(o) : \mathbf{E}_{\perp\sigma}(r, \theta) = \hat{y} \sqrt{2} f_{\sigma} J_n(X_{\sigma} r/a) \sin(n\theta), \quad (3)$$

$$LP_{nm}^x(e) : \mathbf{E}_{\perp\sigma}(r, \theta) = \hat{x} \sqrt{2} f_{\sigma} J_n(X_{\sigma} r/a) \cos(n\theta), \quad (4)$$

$$LP_{nm}^x(o) : \mathbf{E}_{\perp\sigma}(r, \theta) = \hat{x} \sqrt{2} f_{\sigma} J_n(X_{\sigma} r/a) \sin(n\theta), \quad (5)$$

where  $\hat{x}$  and  $\hat{y}$  are unit vectors of  $x$  and  $y$  orthogonal axes in the waveguide cross-section,  $n$  and  $m$  represent the mode numbers, and  $X_\sigma$  is the eigen value of the mode  $\sigma$  with  $(n, m)$ .  $r = \sqrt{x^2 + y^2}$  and  $\theta = \arctan(y/x)$ .  $J_n$  denotes the Bessel-function of the first-kind. The symbol,  $a$ , expresses the radius of the waveguide, and the normalization constant  $f_\sigma$  is

$$f_\sigma = \frac{\sqrt{Z_0}}{a \sqrt{\pi} J_{n+1}(X_\sigma)} = -\frac{\sqrt{Z_0}}{a \sqrt{\pi} J_{n-1}(X_\sigma)}. \quad (6)$$

Generally, a propagating mmw in a corrugated waveguide is expressed as a superposition of several eigen modes  $\sigma$  ( $= 0 \cdots N$ ). Suppose that the miterbends are installed at  $L = L_k$  ( $k = 0, 1, 2, \dots, K - 1$ ). Here  $L$  is the distance along the waveguide axis, and  $L_k$  denotes the distance between the origin,  $O$ , and the center of the  $k$ -th miterbend reflector. The BPM system consists of two BPMs installed in the 90-degree miterbends, for example. Here the type of the miterbends is the same, i.e., both are E-bends or H-bends. The electric field at the position  $(x, y')$  on the  $k$ -th miterbend reflector is described by the following equation:

$$e_{\text{tot}}(x, y', L_k) = \sum_{\sigma=0}^N \sqrt{p_\sigma} \exp\{j(\phi_\sigma - k_\sigma(y' \sin \Phi + L_k))\} \times \mathbf{E}_{\perp\sigma}(x, y' \cos \Phi), \quad (7)$$

where the  $y'$ -axis is on the miterbend reflector plate,  $y' = y/\cos \Phi$ , and  $\Phi$  is the angle between  $y'$ - and  $y$ -axes as shown in Fig. 1. Corresponding to the array of Peltier devices, the reflector surface is divided into  $M \times M$  rectangular sections with the center coordinate of  $(x_i, y'_j)$  and the lengths of  $\Delta x$  and  $\Delta y'$  in  $x$ -,  $y'$ -direction, respectively. The absorbed power in each segment is proportional to

$$|e_{\text{tot}}^D(x_i, y'_j, L_k)|^2 \equiv \int_{x_i - \Delta x/2}^{x_i + \Delta x/2} dx \int_{y'_j - \Delta y'/2}^{y'_j + \Delta y'/2} dy' \times |e_{\text{tot}}(x, y', L_k)|^2, \quad (8)$$

$$x_i = \Delta x \left( i - \frac{M-1}{2} \right) \quad (i = 0, \dots, M-1), \quad (9)$$

$$y'_j = \Delta y' \left( j - \frac{M-1}{2} \right) \quad (j = 0, \dots, M-1). \quad (10)$$

Here, the integrand can be expressed as

$$|e_{\text{tot}}(x, y', L_k)|^2 = \sum_{\sigma=0}^N p_\sigma |\mathbf{E}_{\perp\sigma}(x, y' \cos \Phi)|^2 + \sum_{\substack{\sigma=0 \\ \sigma \neq \tau}}^N \sum_{\tau=0}^N \sqrt{p_\sigma p_\tau} \cos(\phi_{\sigma\tau} - k_{\sigma\tau}(y' \sin \Phi + L_k)) \times \mathbf{E}_{\perp\sigma}(x, y' \cos \Phi) \cdot \mathbf{E}_{\perp\tau}^*(x, y' \cos \Phi), \quad (11)$$

where  $\phi_{\sigma\tau} = \phi_\sigma - \phi_\tau$ ,  $k_{\sigma\tau} = k_\sigma - k_\tau$ . And  $p_\sigma$ ,  $\phi_\sigma$ ,  $k_\sigma$  denote the power, the initial phase, the wave-number of the propagating mode  $\sigma$ , respectively.  $\mathbf{E}_{\perp\sigma}$  corresponds to the electric field given by the equations (2)-(5). The evaluation function  $W_{\text{tot}}$  for determining mode content is defined by

the summation of  $W$  at the miterbend position  $L_k$ , where  $W(L_k)$  is the segment summation of the square value of the difference between the measured  $O$ - and theoretical  $T$ -functions at the miterbend position,  $L_k$ . These are described by the following equations.

$$W_{\text{tot}}(p_\sigma, \phi_\sigma) = \sum_{k=0}^{K-1} W(L_k), \quad (12)$$

where

$$W(L_k) = \sum_{i=0}^{M-1} \sum_{j=0}^{M-1} \{O(x_i, y'_j, L_k) - T(x_i, y'_j, L_k)\}^2, \quad (13)$$

$$T(x_i, y'_j, L_k) = \frac{|e_{\text{tot}}^D(x_i, y'_j, L_k)|^2}{|e_{\text{tot}}^D|_{\text{MAX}}^2}. \quad (14)$$

The mode with  $\sigma = 0$  is assumed to be the  $LP_{01}$  fundamental mode with the initial phase  $\phi_0 = 0$ , and  $\sum_{\sigma=0}^N p_\sigma = 1$ . The sets of  $p_\sigma$  and  $\phi_\sigma$  which minimize the value of  $W_{\text{tot}}(p_\sigma, \phi_\sigma)$  give the ratio of mode content and the initial phase of each mode  $\sigma$ . One of the techniques to minimize  $W_{\text{tot}}$  is proposed in Ref. [2] in detail. A flow chart of the mode analysis is shown in Fig. 4. The analysis consists of two steps. At the first step, the evaluation function,  $W_{\text{tot}}$ , will be minimized for  $LP_{01}$  main mode and one other higher mode of  $LP_{nm}$  by changing initial normalized power to search for the optimum set of power and phase, and to obtain an optimum set  $(p_{\text{opt}}, \phi_{\text{opt}})$  for each mode. Then, at the second step,  $W_{\text{tot}}$ , will be minimized for  $LP_{01}$  main mode and all  $LP_{nm}$  modes using  $p_{\text{opt}}$  and  $\phi_{\text{opt}}$  as the

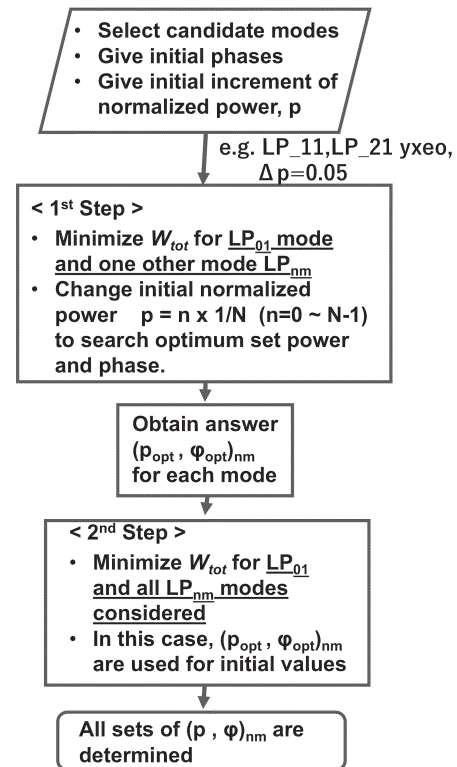


Fig. 4 Flow chart of the propagating mode analysis.

initial values of  $LP_{nm}$  modes. Finally, the optimum set of power and phase can be obtained.

#### 4. Example of Mode Content Analyses Using Artificially Synthesized Data

In order to check the developed code, we prepared the discretized mode-patterns which were artificially synthesized on the mirror-surface of several miterbends using the mixture of given modes. Using the developed code and these patterns, we tried to attempt whether the code could correctly identify the included modes. One example is shown in Fig. 5. The intensity patterns were synthesized by mixing three modes, i.e., 1) the Y-polarized  $LP_{01}$  fundamental mode with 50 % power content and with the initial phase of 0 degree, 2) the Y-polarized  $LP_{11}$  even mode with 20 % power content and with the initial phase of 70 degrees, and 3) the Y-polarized  $LP_{21}$  odd mode with 30 % power content and with the initial phase of 150 degrees. The discretized intensity patterns at  $L = 2$  m, 3 m, and 4 m are shown in Fig. 5. Using these data, several analyses of the contained modes were performed according to the algorithm described in Fig. 4. In this case, two data at  $L = 2$  m and 4 m were used. The results are summarized in Table 2. In addition to the fundamental Y-polarized  $LP_{01}$  main mode, the lowest two modes of  $LP_{11}$  and  $LP_{21}$  with Y- or X-polarization direction and even or odd mode are considered. At the first step, the  $LP_{01}$  main mode and one higher-order mode were considered to minimize the evaluation function of  $W_{tot}$ . The obtained power fraction and phase are shown in Table 2 a). Then, at the second step,

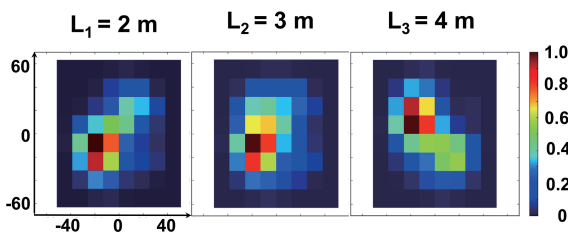


Fig. 5 Examples of the artificially synthesized BPM signals at the three miterbend-positions which are 2, 3, and 4 m apart from the waveguide entrance.

Table 2 Results of mode content analyses using the intensity patterns shown in Fig. 5. The power ratio and phase are listed for a) the first step and b) the second step.

| a) 1st step    |                 |                |               | b) 2nd step     |               |
|----------------|-----------------|----------------|---------------|-----------------|---------------|
| Mode           | $W_{tot}$       | Power ratio    | $\Phi$ (deg.) | Power ratio     | $\Phi$ (deg.) |
| <b>LP11 Ye</b> | <b>3.270965</b> | <b>0.22374</b> | <b>66</b>     | <b>0.193274</b> | <b>69</b>     |
| LP11 Yo        | 5.050816        | 0.043489       | 84            | 0.000009        | 84            |
| LP11 Xe        | 5.80048         | 0              | 179           | 0               | 179           |
| LP11 Xo        | 5.80048         | 0              | 179           | 0.001781        | 179           |
| LP21 Ye        | 5.80048         | 0              | 360           | 0.000004        | 359           |
| <b>LP21 Yo</b> | <b>1.918792</b> | <b>0.60687</b> | <b>134</b>    | <b>0.291717</b> | <b>149</b>    |
| LP21 Xe        | 5.80048         | 0              | 180           | 0.003588        | 180           |
| LP21 Xo        | 5.80048         | 0              | 180           | 0.005325        | 180           |

the minimization of  $W_{tot}$  considering all modes at the same time was performed with the power ratio and the phase which were obtained at the first step as initial values. The obtained results are listed in Table 2 b). The assumed power ratio and phase are correctly obtained within a difference of several percent.

Next, we attempted to confirm the minimum number of the BPM data. The mode content analyses were performed with each data set, i.e., three data at  $L = 2, 3$  and 4 m, two data at  $L = 2$  and 4 m, and one datum at  $L = 4$  m. Generally, the more data that were considered, the better was the accuracy obtained. The accuracy, however, depends on the selection of measured (miterbend) positions and on the beat wavelength of the contained modes. The intensity pattern data at two or more positions are required in order to obtain the higher accuracy.

#### 5. Summary

In a high-power ECRH system for plasma heating, a long-distance and low-loss transmission system of the mmw is required. A real-time monitor of the mmw beam power profile, which can be used in the high-power electromagnetic field of the evacuated and cooled transmission lines, is proposed, designed, and manufactured. The beam position and profile monitor (BPM) consists of an mmw reflector, a Peltier-device array and a heat-sink, which are installed in the reflector-plate of the miterbend. A prototype BPM was constructed and tested using high power mmws. These results show that the BPM can be used as a real-time power profile monitor in the transmission lines of the high-power millimeter-wave. Accordingly, we developed a technique to analyze the propagating modes using the signals of plural BPMs installed in the miterbends in real-time. Using the program, the artificially synthesized mode-mixture could be well analyzed. We are now developing a high performance BPM that can handle the 500 kW power in steady-state, and a feedback control system of a coupling mirror to re-adjust the millimeter-wave beam at the waveguide entrance based on the results obtained by the mode analyses.

#### Acknowledgements

This work is supported by the National Institute for Fusion Science, National Institutes of Natural Sciences, under grant ULRR701, ULRR801, and ULRR804, and is also supported by JSPS KAKENHI Grant Numbers JP21560058, JP24560066, JP16K06940.

- [1] T. Shimozuma, S. Kobayashi, S. Ito *et al.*, J. Infrared mm. THz Waves, **37**, 87 (2016).
- [2] K. Ohkubo, S. Kubo, T. Shimozuma *et al.*, Fusion Sci. Technol. **62**, 389 (2012).
- [3] E.J. Kowalski, J.R. Sirigiri, R.J. Temkin *et al.*, IEEE Trans. Microw. Theory Tech. **58**, 2772 (2010).